

Unsteady MHD Free Convection Flow of Fluid in Microchannel in the Presence of Viscous Dissipation between Vertical Parallel Two Walls

Ahmed D. Abubakar^{1*}, Ibrahim Baba S. Mohammed², Ahmed G. Saleh³

¹Department of Mathematics, Federal University Gashua, Nigeria.

²Department of Mathematics, Federal Polytechnic, Bida, Nigeria.

³Almaarif College of Nursing, Midwifery and Health Sciences Potiskum, Nigeria.

* Corresponding Author

DOI: <https://doi.org/10.51584/IJRIAS.2024.90403>

Received: 27 February 2024; Revised: 14 March 2024; Accepted: 19 March 2024; Published: 26 April 2024

ABSTRACT

Studies of Magnetohydrodynamic (MHD) is very important in industries because of its wide applications in engineering devices such as liquid metal processing, cooling of electronics equipment and power generation. The effect of slip velocity on thermal behaviours of MHD free convection flow over a vertical parallel two walls were presented in this article. The mathematical model include momentum, magnetic field and energy equations. Condition for the existence and uniqueness of solution of the model equations were established using the approach of Lipschitz continuity. The model equations were solved using Olayiwola's generalized polynomial approximation method (OGPAM). The results obtained were presented graphically and discussed. It was observed that increase in Reynolds number and Knudsen number both enhanced the velocity distribution. Also, magnetic field and temperature field were enhanced by magnetic prandtl number and Eckert number respectively.

Keywords and Phrases: MHD, free convection flow, viscous dissipation, Knudsen number, OGPAM.

INTRODUCTION

Magnetohydrodynamic (MHD) is an important area of studies which has its wide applications in power generation, cooling of electrical/electronic equipment and liquid metal processing. A lot of studies have been carried out and findings were reported on MHD free convection flow of fluid in microchannel on a vertical parallel two plates. Free convection slip flow of an exothermic fluid in a convectively heated vertical channel was investigated by Hamza [8]. His numerical simulation show that the formation of flow is strongly dependent on the fluid parameters. Hamza *et al.*[9] studied unsteady MHD free convection flow of an exothermic fluid in a convectively heated vertical channel filled with porous medium. The time-dependent governing equations were analysed numerically using finite difference method. A minor rise in the Hartman number was discovered which slows down the fluid flow.

Uniform transverse magnetic field on the time-dependent free convective fluid flow of a nanofluid with generalized heat transport amongst two parallel plates have been analytically investigated by Ahmed *et al.* [1]. However, Laplace transform technique and fractional derivatives of the Wright's functions were used to obtained the closed form of the temperature field. Moreso, effects of the dimensionless parameters on the nanofluid flow and heat transfer are graphically presented. The integral transform technique is used for finding the exact solutions of the fractional governing differential equations for fluid temperature and velocity field in the work of Hajizadeh *et al.* [7] who considered Free convection flow of nanofluids between two vertical plates with damped heat flux. Analysis of the memory parameter on the velocity and

temperature fields was done, while comparison between the fluid with thermal memory and the ordinary fluid were made. Other related literatures cited in this area include [3, 27, 6].

Jha and Aina [12] analytically presents the impact of induced magnetic field on MHD mixed convection flow in vertical microchannel formed by conducting and non-conducting infinite vertical parallel walls. It was observed that the effect of the induced magnetic field enhanced the velocity profiles compare to the situation of neglecting the magnetic field. Similar studies which considered MHD natural convection flow in vertical microchannel formed by two electrically non-conducting infinite vertical parallel walls was investigated by Jha and Aina [11]. Generally, the findings from their study agreed with the existing literature of Chen and Weng [4]. In a related work of Shu *et al.* [24], fluid velocity slip and temperature jump at a solid surface was investigated.

In a similar studies, Mahjabin and Alim [15] presents the effect of Hartmann number on MHD free convective flow of fluid in a square cavity with a heated cone of different orientation. Their findings shows that Hartman number only have an effect for a large Rayleigh numbers. Moreso, with increasing Ha , heat transfer mode on MHD fluid gradually changes from convection to conduction. Heat transfer analysis of arrhenius-controlled free convective hydromagnetic flow in a micro-channel was investigated by Ojemeru and Hamza [22]. They observed that heat absorption overwhelms fluid flow whereas heat generation creates the opposite condition. In addition, they compared their results with the existing literature written by Jha *et al.* [10]. Ramadan [19] presents both steady and unsteady heat convection in axisymmetric stagnation point flow with momentum and heat slip effects. Their findings established a relation between the specific heat ratio and Prandtl number which characterizes the variation of the Nusselt number with the slip factor.

Dwivedi and Singh [5] investigated unsteady free convective hydromagnetic flow in an infinite vertical cylinder with hall current and heat source. The effects of the dimensionless parameters on both temperature and velocity were graphically presented. However, it was observed that temperature as well as velocity enhances and finally gets to its steady state thereafter. Investigation on the time-dependent free convection MHD of a nanofluid under the influence of radiation and heat generation over a vertical surface was carried out by Rao *et al.* [21]. Numerical solutions of equations governing the flow were obtained by Laplace transform algorithm and symbolic computation software MATLAB. Effects of MHD, heat generation, radiation and nanoparticle volume concentration on the velocity, energy and mass descriptions were shown graphically. The Nusselt number, Sherwood number and skin friction coefficient were also investigated. In a similar work written by Na *et al.* [17], their findings reveal that increasing the value of fractional parameter increased the absolute temperature in the Maxwell fluid flow between vertical walls with damped shear and heat flux. Comparison between ordinary viscous and fractional viscous fluid were also presented graphically.

Investigation by finite difference method on transient laminar natural convective mass transfer stream of an incompressible thick liquid precedent a vertically inclined plate by means of heat source and sink in a MHD radiative medium is considered in the work of Sambath *et al.* [23]. Generally, results from their findings are presented graphically and performs favourably with the existing literatures. In a similar manner, Sobamowo [25] investigated transient free convection thermal and mass transfer of Casson nanofluid over a vertical porous wall exposed to heat radiation and magnetic field. It was established in their report that near the leading edge of the wall, the local Nusselt number is not affected by both buoyancy ratio parameter and Schmidt number. It was also observed that their results will enhance the understanding of transient free convection flow problems under the influence of heat radiation and mass transfer as applied in numerous industrial processes. More so, a thermal optimization through an innovative mechanism of free convection flow of Jeffrey fluid using non-local kernel have been reported by Awan *et al.* [2]. The analytical solutions were obtained through a method of Laplace transform coupled with finite sine-Fourier transform. The behavior of velocity and temperature profiles were also analyzed through numerical computations and graphical representations for different embedded parameters.

Free convective Poiseuille flow through porous medium between two infinite vertical plates in slip flow

regime was studied by Mathur and Mishra [16]. The coupled nonlinear differential equations were solved using perturbation technique and their behaviour is demonstrated via graphs. Findings from their work show a good match with the work of Kalita and Ahmed [13]. Our aim is to study the unsteady MHD free convecton fluid flow in microchannel in the presence of viscous dissipation between vertical parallel two walls which is an extension of Jha and Aina [12].

MODEL FORMULATION

The Unsteady MHD free convecton fluid flow in microchannel in the presence of viscous dissipation between vertical parallel two walls is been considered. A magnetic field of uniform intensity H'_0 is applied on the fluid, perpendicular to the direction of flow. The gravitational force g acts vertically downward. The walls are heated asymmetrically with one wall maintained at a temperature T_1 while the other wall at a temperature T_2 , where $T_1 > T_2$. The x -axis is in the same direction with the gravity g , while y -axis is normal to the walls.

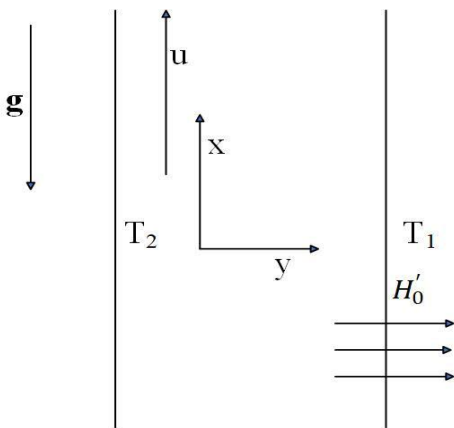


Figure 2.1 Conceptual flow diagram

Based on the above description and assumptions, the equations governing the flow are:

$$\frac{\partial u'}{\partial t'} = \nu \frac{\partial^2 u'}{\partial y'^2} + \frac{\mu_e H'_0}{\rho} \frac{\partial H'}{\partial y'} - \frac{1}{\rho} \frac{\partial P'}{\partial x'} + g\beta(T' - T) \tag{1}$$

$$\frac{\partial H'_0}{\partial t'} = \frac{1}{\sigma \mu_e} \frac{\partial^2 H'_0}{\partial y'^2} + H'_0 \frac{\partial u'}{\partial y'} \tag{2}$$

$$\frac{\partial T'}{\partial t'} = \frac{K}{\rho C_p} \frac{\partial^2 T'}{\partial y'^2} + \frac{\nu}{C_p} \left(\frac{\partial u'}{\partial y'} \right)^2 \tag{3}$$

with the initial and boundary conditions:

$$\begin{aligned} u'(y', 0) = U_0, \quad \left. \frac{2 - \sigma_v}{\sigma_v} \lambda \frac{\partial u'}{\partial y'} \right|_{y=0} - u'(0, t') = 0, \quad \left(\frac{2 - \sigma_v}{\sigma_v} \right) \lambda \left. \frac{\partial u'}{\partial y'} \right|_{y=1} + u'(1, t') = 0 \\ H'(y', 0) = H'_0 y, \quad H'_x(0, t') = 0, \quad \left. \frac{\partial H'_x}{\partial y'} \right|_{y=1} = 0 \\ T'(y', 0) = T_0 y, \quad \left. \frac{2 - \sigma_t}{\sigma_t} \frac{2\gamma}{\gamma + 1} \frac{\lambda}{Pr} \frac{\partial T'}{\partial y'} \right|_{y=0} - T'(0, t') = -T_2, \quad \left. \frac{2 - \sigma_t}{\sigma_t} \frac{2\gamma}{\gamma + 1} \frac{\lambda}{Pr} \frac{\partial T'}{\partial y'} \right|_{y=1} + T'(1, t') = T_1 \end{aligned} \tag{4}$$

METHOD OF SOLUTION

3.1 Dimensional analysis

Dimensionless variables are been introduced as:

$$\left. \begin{aligned} y &= \frac{y'}{b}, \quad t = \frac{U_0 t'}{b}, \quad U = \frac{u'}{U_0}, \quad x = \frac{x'}{b} \\ H &= \frac{\nu H'_x}{b U_0^2} \sqrt{\frac{\mu_e}{\rho}}, \quad P = \frac{P'}{\rho U_0^2}, \quad \theta = \frac{T' - T_0}{T_1 - T_0} \end{aligned} \right\} \quad (5)$$

Substituting (5), into (1) – (4), we obtained in dimensionless form as: $\frac{\partial u}{\partial t} = \frac{1}{Re} \frac{\partial^2 u}{\partial y^2} + M \frac{\partial H}{\partial y} - \frac{\partial P}{\partial x} + Gr\theta$ (6)

$$\frac{\partial H}{\partial t} = \frac{1}{PmRe} \frac{\partial^2 H}{\partial y^2} + \frac{M}{Re^2} \frac{\partial u}{\partial y} \quad (7)$$

$$\frac{\partial \theta}{\partial t} = \frac{1}{Pe} \frac{\partial^2 \theta}{\partial y^2} + \frac{Ec}{Re} \left(\frac{\partial u}{\partial y} \right)^2 \quad (8)$$

$$\begin{aligned} u(y, 0) &= 1, \quad \left. \frac{\partial u}{\partial y} \right|_{y=0} - \phi_0 u|_{y=0} = 0, \quad \left. \frac{\partial u}{\partial y} \right|_{y=1} + \phi_0 u|_{y=1} = 0 \\ H(y, 0) &= l_0 y, \quad H|_{y=0} = 0, \quad \left. \frac{\partial H}{\partial y} \right|_{y=1} = 0 \end{aligned} \quad (9)$$

$$\theta(y, 0) = l_1(y-1), \quad \left. \frac{\partial \theta}{\partial y} \right|_{y=0} - \phi_1 \theta|_{y=0} = -\phi_2, \quad \left. \frac{\partial \theta}{\partial y} \right|_{y=1} + \phi_1 \theta|_{y=1} = \phi_1$$

where,

$$\begin{aligned} Re &= \frac{bU_0}{\nu}, \quad M = \frac{H'_0 b}{\nu} \sqrt{\frac{\mu_e}{\rho}}, \quad Pm = \nu \rho \mu_e, \quad Gr = \frac{g\beta b(T_1 - T_0)}{U_0^2}, \quad Kn = \frac{\lambda}{b}, \quad l_0 = \frac{H'_0 \nu}{b U_0^2} \sqrt{\frac{\mu_e}{\rho}}, \quad l_1 = \frac{T_0}{T_1 - T_0}, \\ \phi_0 &= \frac{1}{\beta_v Kn}, \quad \phi_1 = \frac{1}{\beta_t Kn}, \quad \phi_2 = \frac{\xi}{\beta_t Kn}, \quad \beta_v = \frac{2 - \sigma_v}{\sigma_v}, \quad \beta_t = \frac{2\gamma(2 - \sigma_t)}{(\gamma + 1)\sigma_t Pr}, \\ \xi &= \frac{T_2 - T_0}{T_1 - T_0}. \end{aligned}$$

Nomenclature

- C_p fluid specific heat
- K thermal conductivity
- u dimensionless velocity

H'_0	applied magnetic field
H'_x	dimensional magnetic field
H	dimensionless magnetic field
y	dimensionless distance
t	dimensionless time
g	gravitational acceleration
b	channel width
Re	Reynolds number
Kn	Knudsen number
Pm	magnetic Prandtl number
Gr	Grashof's number
M	Hartman number
U_0	reference velocity
T_0	reference temperature

Greek letters

θ	dimensionless temperature
β	thermal expansion coefficients
μ_e	magnetic permeability
μ	fluid dynamic viscosity
λ	molecular mean free path
ξ	wall-ambient temperature difference ratio
σ	fluid electrical conductivity
ν	fluid kinematic viscosity
ρ	fluid density
β_t, β_v	dimensionless variables
γ	specific thermal ratio

σ_t, σ_v heat and tangential momentum accommodation coefficients, respectively.

3.2 Existence and uniqueness of solutions of the model

Theorem : If $l(y,t,u,H,\theta)$, $m(y,t,u,H,\theta)$, and $n(y,t,u,H,\theta)$ are Lipschitz continuous and $l_0(y)$, $m_0(y)$, and $n_0(y)$ are bounded for $y \in R^n$. Then there exists a unique solution of equations (6) – (8) which satisfy (9).

Proof : We rewrite the equation (6) – (8) as;

$$\frac{\partial u}{\partial t} = \frac{1}{\text{Re}} \frac{\partial^2 u}{\partial y^2} + l(y,t,u,H,\theta), \quad y \in R^n, t > 0, \quad (10)$$

$$\frac{\partial H}{\partial t} = \frac{1}{Pm\text{Re}} \frac{\partial^2 H}{\partial y^2} + m(y,t,u,H,\theta), \quad y \in R^n, t > 0, \quad (11)$$

$$\frac{\partial \theta}{\partial t} = \frac{1}{\text{Re}} \frac{\partial^2 \theta}{\partial y^2} + n(y,t,u,H,\theta), \quad y \in R^n, t > 0, \quad (12)$$

$$u(y,0) = l_0(y), \quad H(y,0) = m_0(y), \quad \theta(y,0) = n_0(y)$$

where

$$l(y,t,u,H,\theta) = M \frac{\partial u}{\partial y} - \frac{\partial P}{\partial x} + Gr\theta \quad m(y,t,u,H,\theta) = \frac{M}{(\text{Re})^2} \frac{\partial u}{\partial y} \quad (13)$$

$$\text{and } n(y,t,u,H,\theta) = \frac{Ec}{\text{Re}} \left(\frac{\partial u}{\partial y} \right)^2$$

For equation (13) to satisfy Lipschitz condition, we must show that

$$\begin{aligned} |l(y,t,u_1,H_1,\theta_1) - l(y,t,u_2,H_2,\theta_2)| &\leq p_1(|u_1 - u_2| + |H_1 - H_2| + |\theta_1 - \theta_2|) \\ |m(y,t,u_1,H_1,\theta_1) - m(y,t,u_2,H_2,\theta_2)| &\leq p_2(|u_1 - u_2| + |H_1 - H_2| + |\theta_1 - \theta_2|), \\ |n(y,t,u_1,H_1,\theta_1) - n(y,t,u_2,H_2,\theta_2)| &\leq p_3(|u_1 - u_2| + |H_1 - H_2| + |\theta_1 - \theta_2|) \end{aligned} \quad (14)$$

from mean value theorem:

$$p_1 = \max\left(\frac{\partial l}{\partial u}, \frac{\partial l}{\partial H}, \frac{\partial l}{\partial \theta}\right), \quad p_2 = \max\left(\frac{\partial m}{\partial u}, \frac{\partial m}{\partial H}, \frac{\partial m}{\partial \theta}\right) \quad \text{and} \quad p_3 = \max\left(\frac{\partial n}{\partial u}, \frac{\partial n}{\partial H}, \frac{\partial n}{\partial \theta}\right) \quad (15)$$

Therefore,

$$p_1 = \max(0, 0, Gr) = Gr, \quad p_2 = \max(0, 0, 0) = 0 \quad \text{and} \quad p_3 = \max(0, 0, 0) = 0.$$

Ignoring the second term at the right hand side, the fundamental solution of equation (10) – (12) are as follows (Toki and Tokis [26]).

$$F(x,t) = \frac{x}{2\pi^{\frac{1}{2}} \left(\frac{1}{\text{Re}}\right)^{\frac{1}{2}} t^{\frac{3}{2}}} \exp\left(-\frac{\text{Re } x}{4t}\right). \quad (16)$$

$$G(x,t) = \frac{x}{2\pi^{\frac{1}{2}} \left(\frac{1}{Pm Re}\right)^{\frac{1}{2}} t^{\frac{3}{2}}} \exp\left(-\frac{Pm Re x}{4t}\right) \tag{17}$$

$$H(x,t) = \frac{x}{2\pi^{\frac{1}{2}} \left(\frac{1}{Re}\right)^{\frac{1}{2}} t^{\frac{3}{2}}} \exp\left(-\frac{Re x}{4t}\right) \tag{18}$$

Clearly, $l(y,t,u,H,\theta)$, $m(y,t,u,H,\theta)$ and $n(y,t,u,H,\theta)$ are Lipschitz continuous. This completes the proof.

3.4 Analytical solution via OGPAM

Suppose

$$\frac{\partial P}{\partial x} = q \exp(-\sigma t) \tag{20}$$

and let $0 < M \ll 1$, $Gr = rM$

such that

$$\left. \begin{aligned} u(y,t) &= u_0(y,t) + Mu_1(y,t) + \dots \\ H(y,t) &= H_0(y,t) + MH_1(y,t) + \dots \\ \theta(y,t) &= \theta_0(y,t) + M\theta_1(y,t) + \dots \end{aligned} \right\} \tag{21}$$

equations (6) – (9) were solve analytically using OGPAM (Olayiwola, [18]), and obtained as follows:

$$u(y,t) = (u_0|_{y=1} + \phi_0 u_0|_{y=1} y - \phi_0 u_0|_{y=1} y^2) + M(u_1|_{y=1} + \phi_0 u_1|_{y=1} y - \phi_0 u_1|_{y=1} y^2) \tag{22}$$

$$H(y,t) = (2l_0 \exp(-l_{15}t)y^2 - l_0 \exp(-l_{15}t)y^3) + M(2ky - ky^2) \tag{23}$$

$$\theta(y,t) = (\theta_0|_{y=1} + l_{16} + (\phi_1 \theta_0|_{y=1} + l_{17})y + (-\phi_1 \theta_0|_{y=1} + l_{18})y^2) + M(\theta_1|_{y=1} + \phi_1 \theta_1|_{y=1} y - \phi_1 \theta_1|_{y=1} y^2) \tag{24}$$

where

$$u_0|_{y=1} = l_4 \exp(-\sigma t) + l_5 \exp(-l_2 t),$$

$$\theta_0|_{y=1} = l_{25}(1 - \exp(-l_{20}t)) + l_{26}(\exp(-2\sigma t) - \exp(-l_{20}t)) + l_{27}(\exp(-(l_2 + \sigma)t) - \exp(-l_{20}t)) + l_{28}(\exp(-2l_2t) - \exp(-l_{20}t))$$

$$u_1|_{y=1} = l_{41}(\exp(-l_{15}t) - \exp(-l_2t)) + l_{42}(1 - \exp(-l_2t)) + l_{43}(\exp(-l_{20}t) - \exp(-l_2t)) + l_{44}(\exp(-2\sigma t) - \exp(-l_2t)) + l_{45}(\exp(-(l_2 + \sigma)t) - \exp(-l_2t)) + l_{46}(\exp(-2l_2t) - \exp(-l_2t))$$

$$\begin{aligned} \theta_1|_{y=1} = & l_{48}(\exp(-2l_{15}t) - \exp(-l_{20}t)) + l_{49}(1 - \exp(-l_{20}t)) + l_{50}(\exp(-2l_{20}t) - \exp(-l_{20}t)) + \\ & l_{51}(\exp(-4\sigma) - \exp(-l_{20}t)) + l_{52}(\exp(-2(l_2 + \sigma)t) - \exp(-l_{20}t)) + \\ & l_{53}(\exp(-4l_2t) - \exp(-l_{20}t)) + l_{54}(\exp(-2l_2t) - \exp(-l_{20}t)) + l_{55}(\exp(-l_{15}t) - \exp(-l_{20}t)) \\ & + l_{56}(\exp(l_{20} - l_{15})t - \exp(-l_{20}t)) + l_{57}(\exp(-(l_{15} + 2\sigma)t) - \exp(-l_{20}t)) + \\ & l_{58}(\exp(-(l_{15} + l_2 + \sigma)t) - \exp(-l_{20}t)) + l_{59}(\exp(-(l_{15} + 2l_2)t) - \exp(-l_{20}t)) - \\ & l_{60}(\exp(-(l_{15} + l_2)t) - \exp(-l_{20}t)) + l_{61}t + l_{62}(\exp(-2\sigma) - \exp(-l_{20}t)) + \\ & l_{63}(\exp(-(l_2 + \sigma)t) - \exp(-l_{20}t)) - l_{64}(\exp(-l_2t) - \exp(-l_{20}t)) + \\ & l_{65}(\exp(-(l_{20} + 2\sigma)t) - \exp(-l_{20}t)) + l_{66}(\exp(-(l_{20} + l_2 + \sigma)t) - \exp(-l_{20}t)) + \\ & l_{67}(\exp(-(l_{20} + 2l_2)t) - \exp(-l_{20}t)) - l_{68}(\exp(-(l_{20} + l_2)t) - \exp(-l_{20}t)) + \\ & l_{69}(\exp(-(l_2 + 3\sigma)t) - \exp(-l_{20}t)) - l_{70}(\exp(-(2\sigma + l_2)t) - \exp(-l_{20}t)) + \\ & l_{71}(\exp(-(\sigma + 3l_2)t) - \exp(-l_{20}t)) - l_{72}(\exp(-(\sigma + 2l_2)t) - \exp(-l_{20}t)) - \\ & l_{73}(\exp(-3l_2t) - \exp(-l_{20}t)) \end{aligned}$$

$$l_0 = \frac{H'_0\nu}{bU_0^2} \sqrt{\frac{\mu_e}{\rho}}, \quad l_1 = \frac{T_0}{T_1 - T_0}, \quad l_2 = \frac{12\phi_0}{\text{Re}(6 + \phi_0)}, \quad l_3 = \frac{6q}{6 + \phi_0}, \quad l_4 = \frac{-l_3}{l_2 - \sigma}, \quad l_5 = 1 - l_4, \quad l_6 = \phi_0 l_4,$$

$$l_7 = \phi_0 l_3, \quad l_8 = 2\phi_0 l_4, \quad l_9 = 2\phi_0 l_5, \quad l_{10} = l_6 l_7, \quad l_{11} = l_6 l_8, \quad l_{12} = l_6 l_9, \quad l_{13} = l_7 l_9, \quad l_{14} = l_8 l_9, \quad l_{15} = \frac{1}{Pm \text{Re}},$$

$$l_{16} = \left(\frac{\phi_2}{2} - \frac{\phi_1 \phi_2}{4 + 2\phi_1} - \frac{\phi_1}{2} + \frac{\phi_1 \phi_1}{4 + 2\phi_1} \right), \quad l_{17} = \left(-\phi_2 + \frac{\phi_1 \phi_2}{2 + \phi_1} - \frac{\phi_1 \phi_1}{2 + \phi_1} \right), \quad l_{18} = \left(\frac{\phi_2}{2} - \frac{\phi_1 \phi_2}{4 + 2\phi_1} + \frac{\phi_1}{2} + \frac{\phi_1 \phi_1}{4 + 2\phi_1} \right),$$

$$l_{19} = \frac{Ec}{\text{Re}}, \quad l_{20} = \frac{12\phi_1}{Pe(6 + \phi_1)}, \quad l_{21} = \frac{1}{Pe} \left(\phi_2 - \frac{\phi_1 \phi_2}{2 + \phi_1} - \phi_1 - \frac{\phi_1 \phi_1}{2 + \phi_1} \right), \quad l_{22} = \frac{6 + \phi_1}{6}, \quad l_{23} = \frac{l_{21}}{l_{22}}, \quad l_{24} = \frac{l_{19}}{l_{22}},$$

$$l_{25} = \frac{l_{23}}{l_{20}}, \quad l_{26} = \frac{1}{l_{20} - 2\sigma} \left(l_{24} l_6^2 + \frac{l_{24} l_{11}}{2} + \frac{l_{24} l_8^2}{3} \right), \quad l_{27} = \frac{1}{l_{20} - l_2 - \sigma} \left(l_{24} l_{10} + \frac{l_{24} l_{12}}{2} + \frac{l_{24} l_{13}}{3} \right),$$

$$l_{28} = \frac{1}{l_{20} - 2l_2} \left(l_{24} l_7^2 + \frac{l_{24} l_{13}}{2} + \frac{l_{24} l_9^2}{3} \right), \quad l_{29} = l_0, \quad l_{30} = rl_{25} + rl_{16} + \frac{r\phi_1 l_{25}}{2} + \frac{rl_{17}}{2} - \frac{r\phi_1 l_{25}}{3} + \frac{rl_{18}}{3},$$

$$l_{31} = \frac{r\phi_1 l_{11}}{12} + \frac{r\phi_1 l_{28}}{3} + \frac{r\phi_1 l_{27}}{3} + \frac{r\phi_1 l_{26}}{3} + \frac{r\phi_1 l_{25}}{3} - \frac{r\phi_1 l_{11}}{6} - \frac{r\phi_1 l_{28}}{2} - \frac{r\phi_1 l_{27}}{2} - \frac{r\phi_1 l_{26}}{2} - \frac{r\phi_1 l_{25}}{2} - \frac{rl_1}{2} - rl_{28} - rl_{27} - rl_{26} - rl_{25},$$

$$l_{32} = rl_{26} + \frac{r\phi_1 l_{26}}{2} - \frac{r\phi_1 l_{26}}{3}, \quad l_{33} = rl_{27} + \frac{r\phi_1 l_{27}}{2} - \frac{r\phi_1 l_{27}}{3}, \quad l_{34} = rl_{28} + \frac{r\phi_1 l_{28}}{2} + \frac{r\phi_1 l_{28}}{3}, \quad l_{35} = \frac{6l_{29}}{6 + \phi_0},$$

$$l_{36} = \frac{6l_{30}}{6 + \phi_0}, \quad l_{37} = \frac{6l_{31}}{6 + \phi_0}, \quad l_{38} = \frac{6l_{32}}{6 + \phi_0}, \quad l_{39} = \frac{6l_{33}}{6 + \phi_0}, \quad l_{40} = \frac{6l_{34}}{6 + \phi_0}, \quad l_{41} = \frac{l_{35}}{l_2 - l_{15}}, \quad l_{42} = \frac{l_{36}}{l_2},$$

$$l_{43} = \frac{l_{37}}{l_2 - l_{20}}, \quad l_{44} = \frac{l_{38}}{l_2 - 2\tau}, \quad l_{45} = -\frac{l_{39}}{\tau}, \quad l_{46} = -\frac{l_{40}}{l_2},$$

$$l_{47} = \phi_0 l_{41} + \phi_0 l_{42} + \phi_0 l_{43} + \phi_0 l_{44} + \phi_0 l_{45} + \phi_0 l_{46}, \quad l_{48} = \frac{\phi_0^2 l_{24} l_{41}^2}{3(l_{20} - 2l_{15})}, \quad l_{49} = \frac{\phi_0^2 l_{24} l_{42}^2}{3l_{20}}, \quad l_{50} = \frac{\phi_0^2 l_{24} l_{43}^2}{3l_{20}},$$

$$l_{51} = \frac{\phi_0^2 l_{24} l_{44}^2}{3(l_{20} - 4\sigma)}, \quad l_{52} = \frac{\phi_0^2 l_{24} l_{45}^2 + 2\phi_0^2 l_{24} l_{44} l_{46}}{3(l_{20} - 2l_2 - 2\sigma)}, \quad l_{53} = \frac{\phi_0^2 l_{24} l_{46}^2}{3(l_{20} - 4l_2)}, \quad l_{54} = \frac{l_{24} l_{47}^2 + 2\phi_0^2 l_{24} l_{42} l_{46}}{3(l_{20} - 2l_2)},$$

$$l_{55} = \frac{2\phi_0^2 l_{24} l_{44} l_{42}}{3(l_{20} - l_{15})}, \quad l_{56} = \frac{2\phi_0^2 l_{24} l_{41} l_{42}}{3(l_{20} - l_{15})}, \quad l_{57} = \frac{2\phi_0^2 l_{24} l_{41} l_{44}}{3(l_{20} - l_{15} - 2\sigma)}, \quad l_{58} = \frac{2\phi_0^2 l_{24} l_{41} l_{45}}{3(l_{20} - l_{15} - l_2 - \sigma)},$$

$$l_{59} = \frac{2\phi_0^2 l_{24} l_{41} l_{46}}{3(l_{20} - l_{15} - 2l_2)}, \quad l_{60} = \frac{\phi_0 l_{24} l_{41} l_{47}}{3(l_{20} - l_{15} - l_2)}, \quad l_{61} = \frac{2\phi_0^2 l_{24} l_{42} l_{43}}{3}, \quad l_{62} = \frac{2\phi_0^2 l_{24} l_{42} l_{44}}{3(l_{20} - 2\sigma)},$$

$$l_{63} = \frac{2\phi_0^2 l_{24} l_{42} l_{45}}{3(l_{20} - l_2 - \sigma)}, \quad l_{64} = \frac{\phi_0 l_{24} l_{42} l_{47}}{3(l_{20} - l_2)}, \quad l_{65} = \frac{2\phi_0^2 l_{24} l_{43} l_{44}}{6\sigma}, \quad l_{66} = \frac{2\phi_0^2 l_{24} l_{43} l_{45}}{3(l_2 + \sigma)},$$

$$l_{67} = \frac{2\phi_0^2 l_{24} l_{43} l_{46}}{6l_2}, \quad l_{68} = \frac{\phi_0 l_{24} l_{43} l_{47}}{3l_2}, \quad l_{69} = \frac{2\phi_0^2 l_{24} l_{44} l_{45}}{3(l_{20} - l_2 - 3\sigma)}, \quad l_{70} = \frac{\phi_0 l_{24} l_{44} l_{47}}{3(l_{20} - l_2 - 2\sigma)},$$

$$l_{71} = \frac{2\phi_0^2 l_{24} l_{45} l_{46}}{3(l_{20} - 3l_2 - \sigma)}, \quad l_{72} = \frac{\phi_0 l_{24} l_{45} l_{47}}{3(l_{20} - 2l_2 - \sigma)}, \quad l_{73} = \frac{\phi_0 l_{24} l_{46} l_{47}}{3(l_{20} - 3l_2)}.$$

RESULTS AND DISCUSSION

Mixed convection viscous flow of fluid has been considered in a vertical microchannel walls. Simulation was carried out to show the effects of the governing parameters by employing Olayiwola's Generalized Polynomial Approximation Method (OGPAM) on the equations (6) – (9) which were graphically presented. The solutions are computed for the different values of

$$\beta_i = 1, \quad \beta_v = 1, \quad Gr = 0.3, \quad M = 0.01, \quad Ec = 0.2, \quad R_e = 4, \quad P_e = 0.5, \quad Pm = 0.5, \quad Kn = 0.05, \quad y = 1, \quad t = 1,$$

$$\xi = 1, \quad q = 1, \quad \sigma = 0.001. \text{ using computer symbolic algebraic package MAPLE 2021 version.}$$

Figure 4.1 and 4.2 show the effects of Reynolds number on velocity distribution against distance and time, Reynolds number is the ratio of inertial to viscous forces. It was observed from these figures that Reynolds number increased the fluid velocity.. Figure 4.3, 4.4, 4.9 and 4.10 presents the impact of Knudsen number. The Knudsen number enhance the velocity distribution and reduced temperature both along distance and time. This type of behaviour of Knudsen number has also been observed by Rashid *et al.* [20] who investigated the significance of Knudsen number and corrugation on EMHD flow under metallic nanoparticles impact. In figure 4.5 and 4.6, Magnetic pranditl number increased magnetic field within the fluid. Similarly, as the value of Eckert number increases, the temperature of the fluid increases with distance and time wich can be seen in figure 4.7 and 4.8. This is due to an increase in friction inside the fluid which transforms the mechanical energy into heat energy. Similar findings have been reported by Khan and Alzahrani [14] who studied Carreau–Yasuda fluid under Entropy-optimized dissipative flow with radiative thermal flux and chemical reaction.

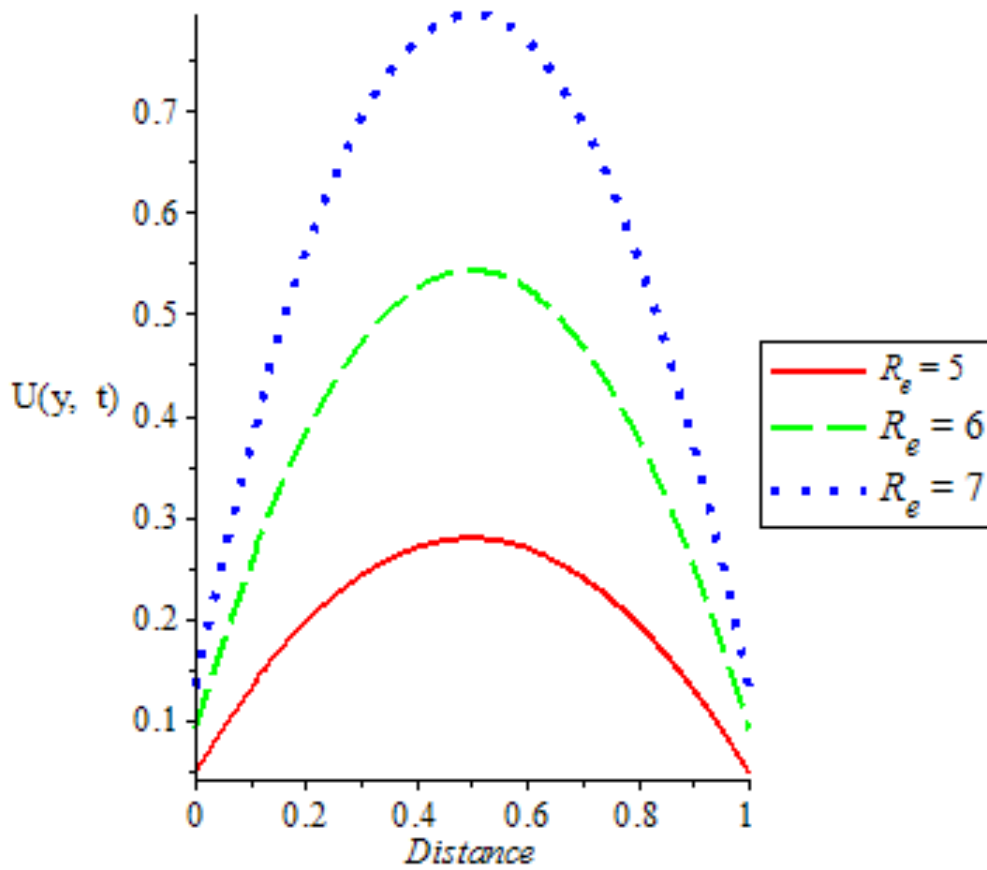


Figure 4.1: Effect of variation of velocity distribution with Reynolds number against distance.

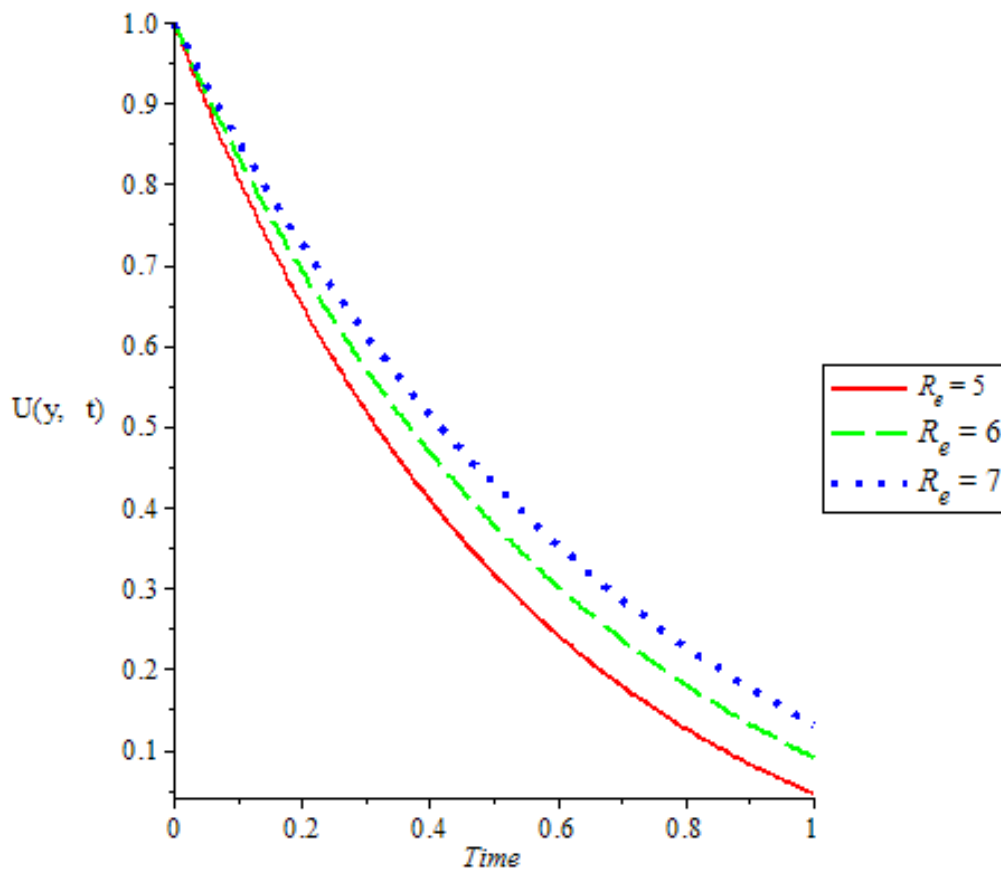


Figure 4.2: Effect of variation of velocity distribution with Reynolds number against time.

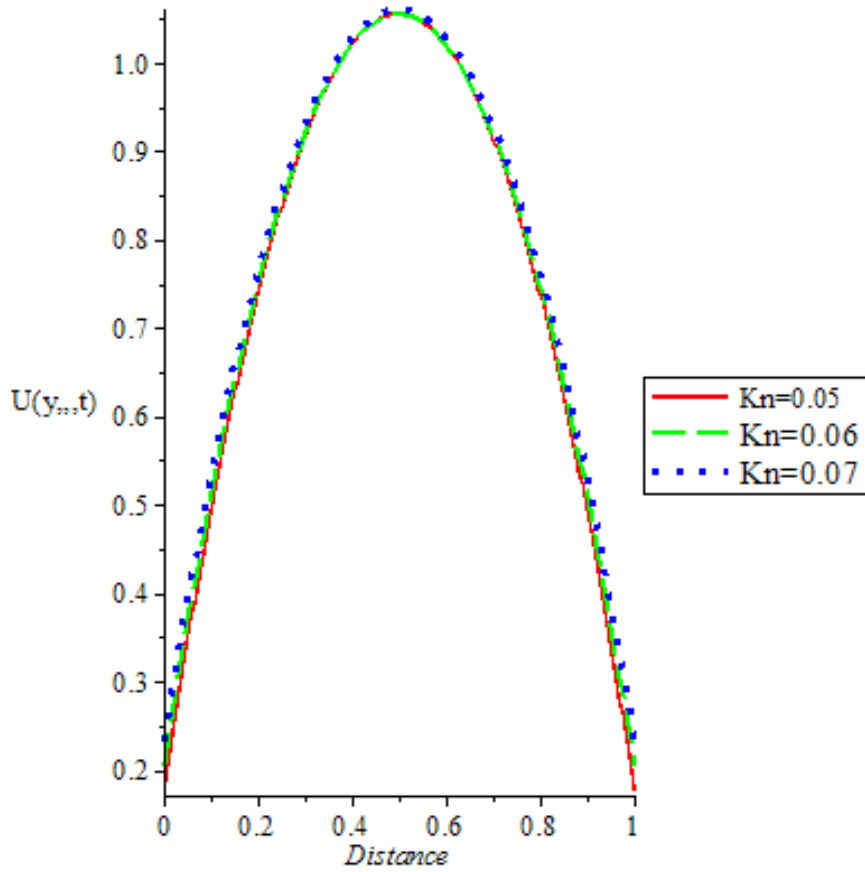


Figure 4.3: Effect of variation of velocity distribution with Knudsen number against distance.

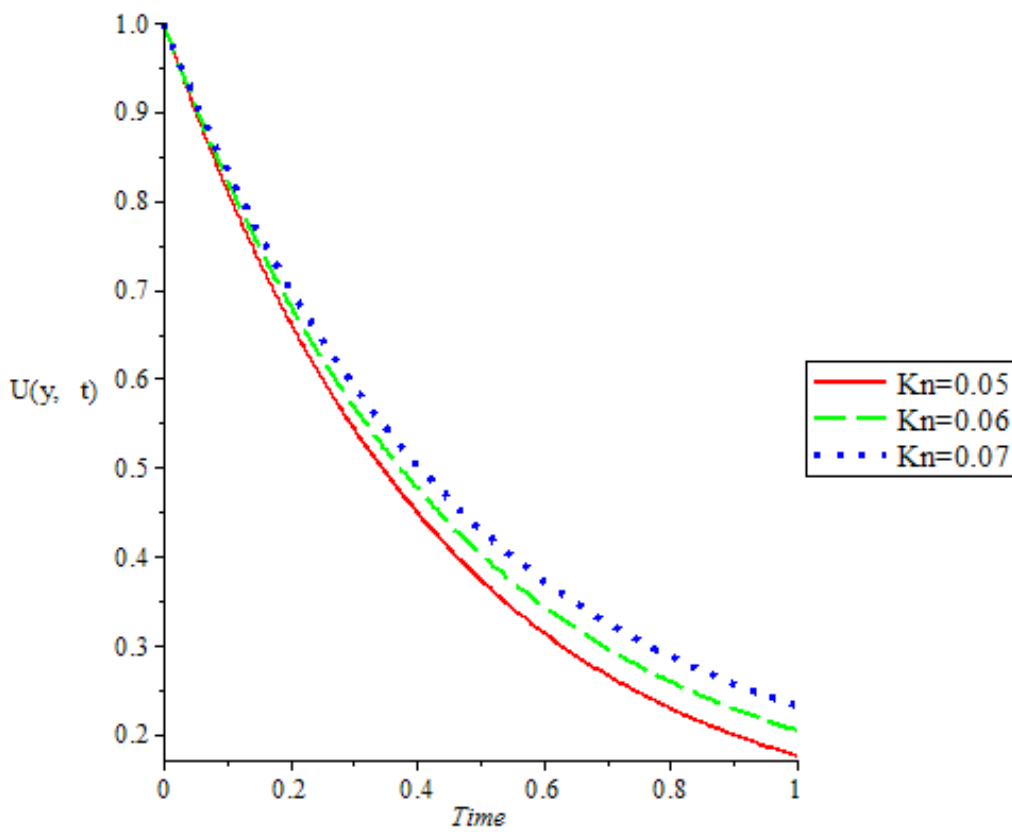


Figure 4.4: Effect of variation of velocity distribution with Knudsen number time.

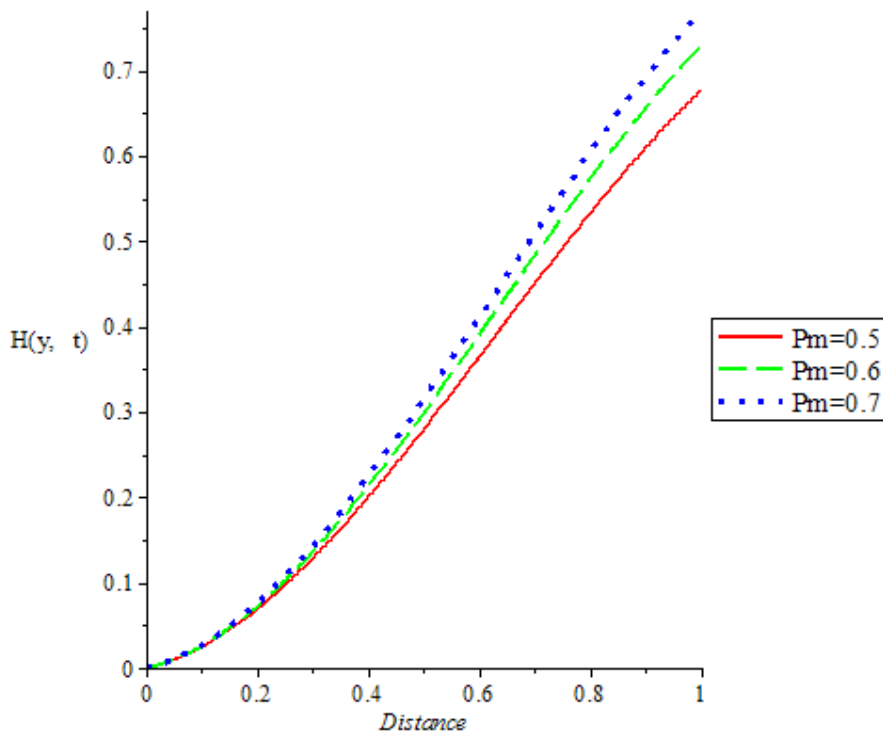


Figure 4.5: Effect of variation of magnetic field with magnetic Prandtl number distance.

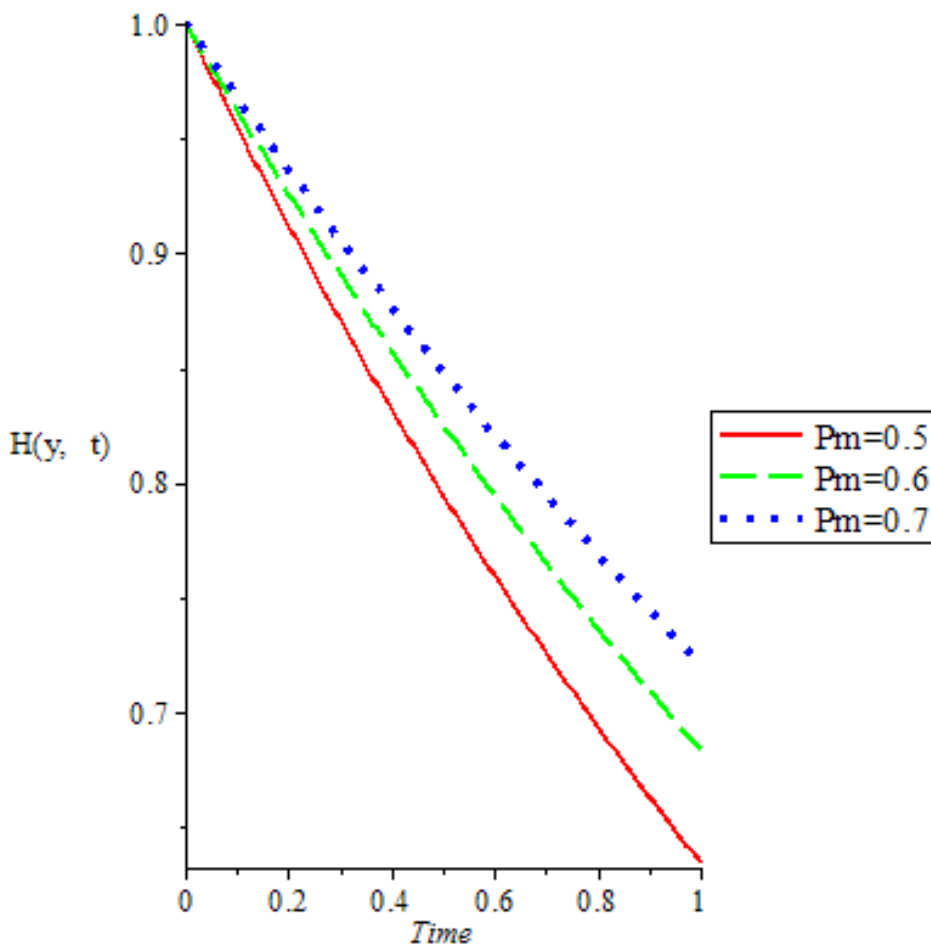


Figure 4.6: Effect of variation of magnetic field with magnetic Prandtl number time.

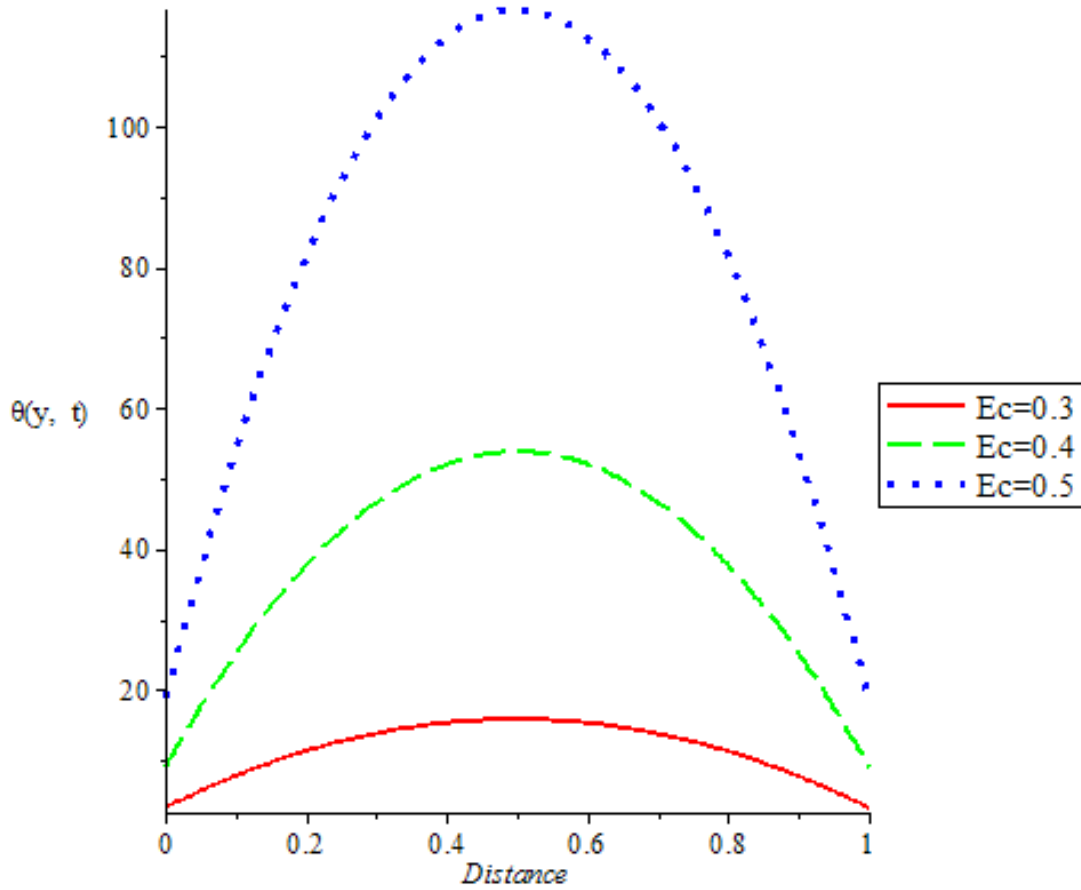


Figure 4.7: Effect of variation of temperature distribution with Eckert number against distance.

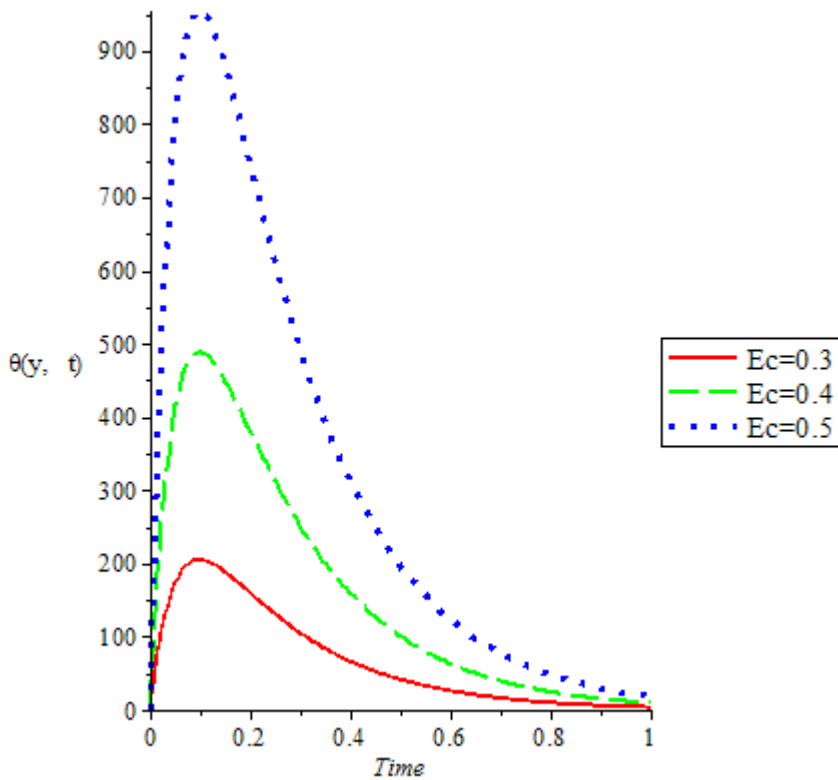


Figure 4.8: Effect of variation of temperature distribution with Eckert number against time.

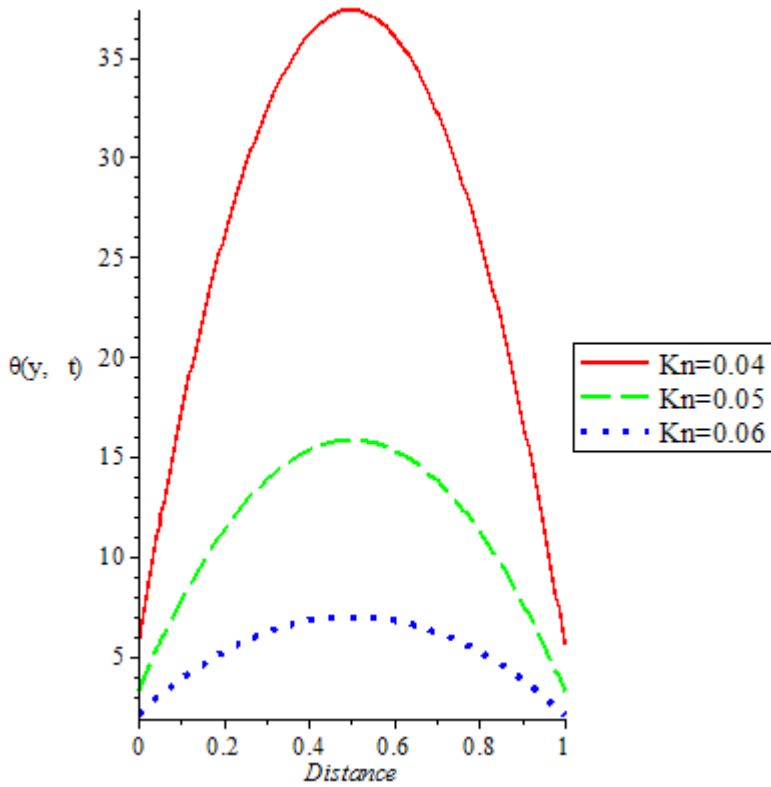


Figure 4.9: Effect of variation of temperature distribution with Knudsen number against distance.

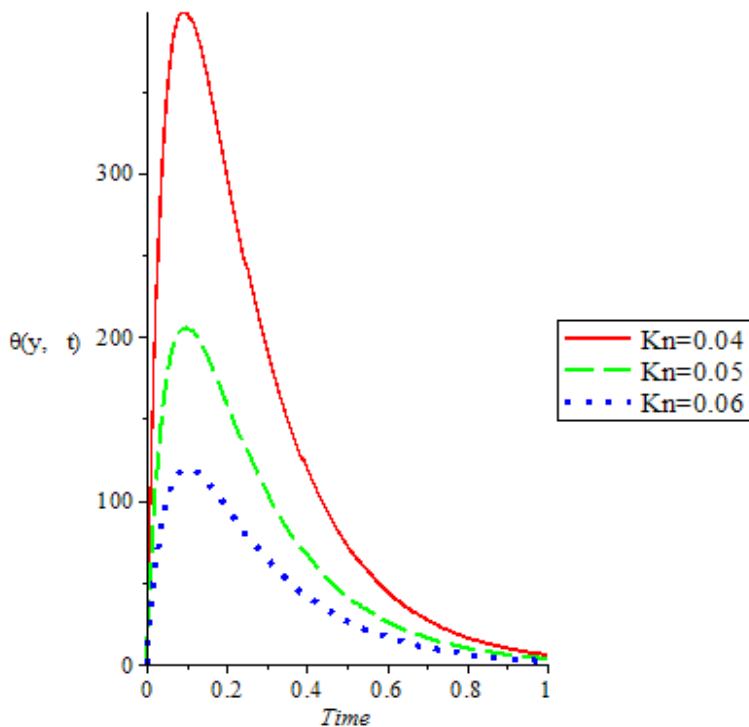


Figure 4.10: Effect of variation of temperature distribution with Knudsen number against time.

CONCLUSION

The magnetohydrodynamic of free convection flow of fluid in microchannel in the presence of viscous dissipation between vertical parallel two walls was investigated analytically. The condition for the existence and uniqueness of solution of the model equations were established using the approach of

Lipschitz continuity. Effects of flow parameters on the velocity profile, magnetic field and temperature profile are graphically presented and we concluded as follows:

1. It was found that increase in Reynolds number increased the velocity profile and thereafter reduced with time.
2. Increase in Knudsen number enhanced the velocity distribution and decreased the temperature profile.
3. Magnetic Prandtl number increased magnetic field and at later time reduced the magnetic field.
4. Temperature of the fluid flow increases with distance and time, as the value of Eckert number increases.

COMPETING INTERESTS

None.

REFERENCES

1. Ahmed, N., Shah, N. A., Ahmad, B., Shah, S. I. A., Ulhaq, S. & Rahimi-Gorji, M. Transient MHD convective flow of fractional nanofluid between vertical plates. *Journal of Applied and Computational Mechanics*, 5(4), (2019), 592-602, DOI: 10.22055/JACM.2018.26947.1364.
2. Awan, A. U., Ali, Q., Riaz, S., Shah, N. A., & Chung, J. D. A thermal optimization through an innovative mechanism of free convection flow of Jeffrey fluid using non-local kernel. *Case Studies in Thermal Engineering*, 24, (2021), 100851.
3. Buonomo, B. and Manca, O. Natural Convection Flow in a Vertical Micro-Channel with Heated at Uniform Heat Flux, *International Journal of Thermal Science*, 49, (2012), 1333–1344.
4. Chen, C. K. & Weng, H. C. Natural convection in a vertical microchannel, *Journal of heat transfer*. 127, (2005), 1053–1056.
5. Dwivedi, N. & Singh, A. K. Transient free convective hydromagnetic flow in an infinite vertical cylinder with hall current and heat source/sink. *Heat Transfer-Wiley*, 1-18, (2020), DOI: 10.1002/htj.21818.
6. Gambo, D., Yusuf, T. S., Oluwagbemiga, S. A., Kozah, J. D. & Gambo, J. J. Analysis of free convective hydromagnetic flow of heat generating/absorbing fluid in an annulus with isothermal and adiabatic boundaries, *Partial Differential Equations in Applied Mathematics*, (2021), <https://doi.org/10.1016/j.padiff.2021.100080>.
7. Hajizadeh, A., Shah, N. A., Syed Inayat Ali Shah, S. I. A., Animasaun, I. L., Rahimi-Gorji, M. & Alarifi, I. M. Free convection flow of nanofluids between two vertical plates with damped thermal flux. *Journal of Molecular Liquids*, 289, (2019), 110964.
8. Hamza, M. M. Free convection slip flow of an exothermic fluid in a convectively heated vertical channel. *Ain Shams Engineering Journal*, 9, (2016), 1313 – 1323 <http://dx.doi.org/10.1016/j.asej.2016.08.011>.
9. Hamza, M. M., Shuaibu, A. & Kamba, S. A. Unsteady MHD free convection flow of an exothermic fluid in a convectively heated vertical channel filled with porous medium. *Scientific Report*. (2022), 12:11989 | <https://doi.org/10.1038/s41598-022-16064-y>.
10. Jha, B. K. Aina, B. & Ajiya, A. T. MHD natural convection flow in a vertical parallel plate microchannel. *Ain shams Eng Journal*. 6, (2014), 289–295.
11. Jha, B. K. & Aina, B. Role of induced magnetic field on MHD natural convection flow in vertical microchannel formed by two electrically non-conducting infinite vertical parallel plates. *Alexandria Engineering Journal*, 55, (2016), 2087–2097.
12. Jha, B. K. & Aina, B. Impact of induced magnetic field on MHD mixed convection flow in vertical microchannel formed by non-conducting and conducting infinite vertical parallel plates. *Journal of Nanofluid*, 6, (2017), 1–11.
13. Kalita, D., & Ahmed, N. Transient MHD Free Convection from an Infinite Vertical Porous Plate in a Rotating Fluid with Mass Transfer and Hall Current. *Journal of Energy, Heat and Mass Transfer*, 33(1), (2011), 271-292.

14. Khan, M. I. & Alzahrani, F. Entropy-optimized dissipative flow of Carreau–Yasuda fluid with radiative heat flux and chemical reaction, *European Physical Journal Plus*, (2020), 135:516, <https://doi.org/10.1140/epjp/s13360-020-00532-3>.
15. Mahjabin, S. & Alim, M. A. Effect of Hartmann number on free convective flow of MHD fluid in a square cavity with a heated cone of different orientation. *American Journal of Computational Mathematics*, 8, (2018), 314-325, <http://www.scirp.org/journal/ajcm>.
16. Mathur, P., & Mishra, S. R. Free convective Poiseuille flow through porous medium between two infinite vertical plates in slip flow regime *Pramana – Journal of Physics*, (2020), 94:69, <https://doi.org/10.1007/s12043-020-1916-y>.
17. Na, W., Shah, N. A., Tlili, I., & Siddique, I. Maxwell fluid flow between vertical plates with damped shear and thermal flux: Free convection. *Chinese Journal of Physics*, 65, (2020), 367-376.
18. Olayiwola, R. O. Solving parabolic equations by Olayiwola's generalized polynomial approximation method. *International Journal of Mathematical Analysis and Modelling*, 5(3), (2022), 24 - 43.
19. Ramadan, K. M. Slip effects on steady and transient stagnation-point heat transfer in axisymmetric geometries. *Journal of Mechanical Engineering Science*, 228(15), (2014), 2765–2777.
20. Rashid, M., Shahzadi, I. & Nadeem, S. Significance of Knudsen number and corrugation on EMHD flow under metallic nanoparticles impact, *Physica A*, 551, (2020), 124089.
21. Rao, P. S., Prakash, Om., Mishra, S. R., & Sharma, R. P. The transient free convection magnetohydrodynamic motion of a nanofluid over a vertical surface under the influence of radiation and heat generation. *Indian Journal of Geo Marine Sciences*, 49 (05), (2020), 889-897.
22. Ojemer, G. & Hamza, M. M. Heat transfer analysis of arrhenius-controlled free convective hydromagnetic flow with heat generation/absorption effect in a micro-channel. *Alexandria Engineering Journal*, 61, (2022), 12797–12811.
23. Sambath, P. Pullepu, B., & Kannan R. M. Unsteady free convective MHD radiative mass transfer flow past from an inclined vertical plate with heat source and sink. *AIP Conference Proceedings* 2112, (2019), 020005, <https://doi.org/10.1063/1.5112190>.
24. Shu, J. J., Teo, J. B. M. & Chan, W. K. Fluid Velocity Slip and Temperature Jump at a Solid Surface. *Applied Mechanics Reviews*. (2017), doi:10.1115/1.4036191.
25. Sobamowo, M. G. Transient free convection heat and mass transfer of Casson nanofluid over a vertical porous plate subjected to magnetic field and thermal radiation. *Engineering and Applied Science Letters*, 3(2), (2020), 9-18; doi:10.30538/psrp-easl2020.0037.
26. Toki C. J. and Tokis J. N. Exact solutions for the unsteady free convection flows on a porous plate with time dependent heating. *ZAMM Journal of Applied Mathematics and Mechanics*, 87, (2007). 4 – 13.
27. Weng, H. C. and Chen, C. K. Drag reduction and heat transfer enhancement over a heated wall of a vertical annular micro-channel, *International Journal of Heat and Mass Transfer*, 52, (2009), 1075–1079.